Investigation of the physics and control of HL-2M advanced divertor

G.Y. Zheng[1], X.R. Duan[1], B. Li[1], X.Q. Xu[3], H.L. Du[1], D. Humphreys[2], H.Y. Guo[2], J.X. Li[1], B.J. Xia[4], L. Lao[2], M. Xue[1], S. Wang[1], L. Xue[1], M. Walker[2], J. Leuer[2], Y.Q. Liu[2], O. Meneghini[2], and Q.P. Yuan[4]

[1]Southwestern Institute of Physics, P.O. Box 432, Chengdu, People's Republic of China

[2]General Atomics, PO Box 85608, San Diego, California 92186-5608, USA

[3]Lawrence Livermore National Laboratory, Livermore, CA 94550, USA

[4]Institute of Plasma Physics, Chinese Academy of Science, Hefei, People's Republic of China

US: March 22-26, 2021 / PRC: March 23-27, 2021

HL-2M Tokamak

HL-2M Mission: Addressing crucial physics and technology issue for ITER /CFETR / next-step fusion device

- High performance, high β_N scenarios compatible with various divertor configurations
- Tests and validation of high heat flux plasma-facing components
- Investigation of burning plasma physics

Main parameters

Plasma current	Ip = 2.5 MA
Major radius	R = 1.78 m
Minor radius	a = 0.65 m
Aspect ratio	R/a = 2.8
Elongation	K = 1.8-2
Triangularity	δ > 0.5
Toroidal field	B_T = 2.2 (3) T
Flux swing	ΔΦ= 14Vs
Heating power	25 MW

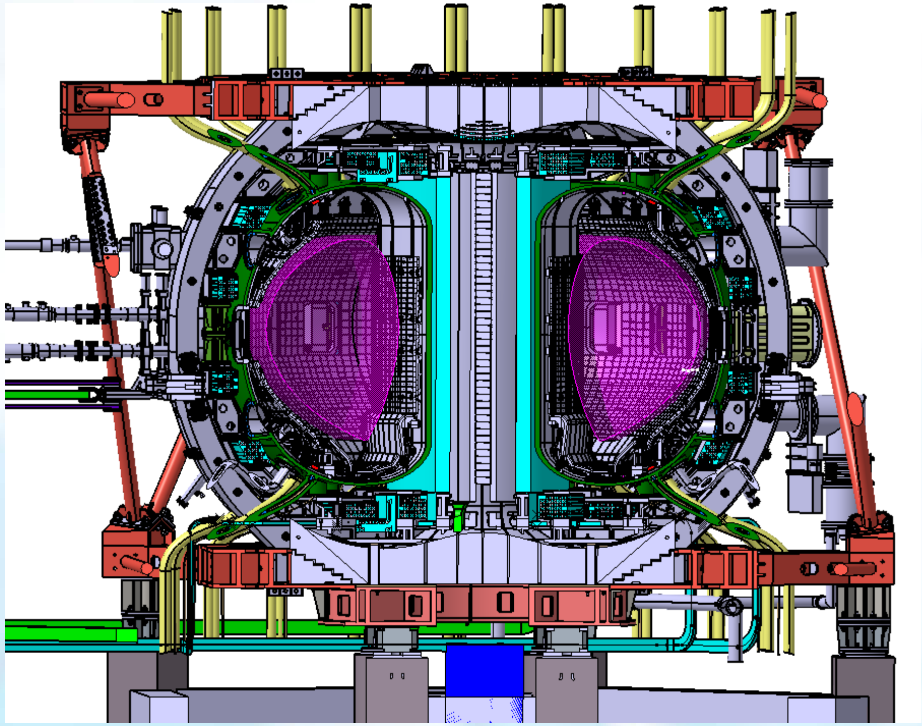

- ❑ Neutral Beam Heating
  - ✓ 5+5+5 MW (80keV for D_2 / 55keV for H_2)
  - ✓ Co (2) & counter(1) injection
  - ✓ ITER-like Cryopump
- ❑ Electron Resonance Frequency Heating
  - ✓ 6MW (105GHz) + 2MW (105/140GHz)
  - ✓ 6MW equatorial launcher
  - ✓ 2MW upper launcher
- ❑ Lower Hybrid Current Drive 2 (4) MW (3.7GHz)
  - ✓ Fully Active Multi-junction launcher
  - ✓ Peak parallel refractive index $N_{//}(0)$= 2.25

HL-2M divertor

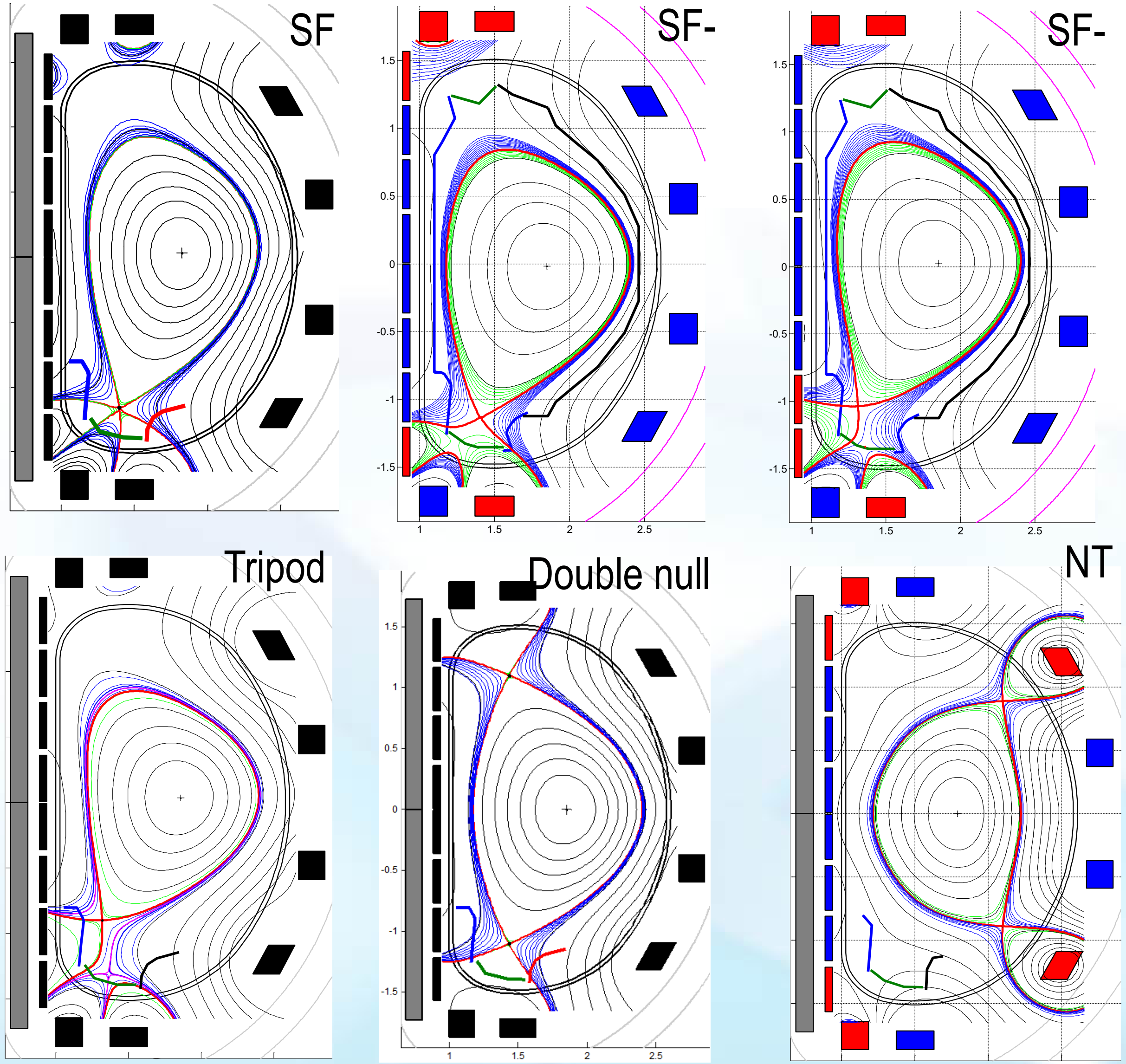

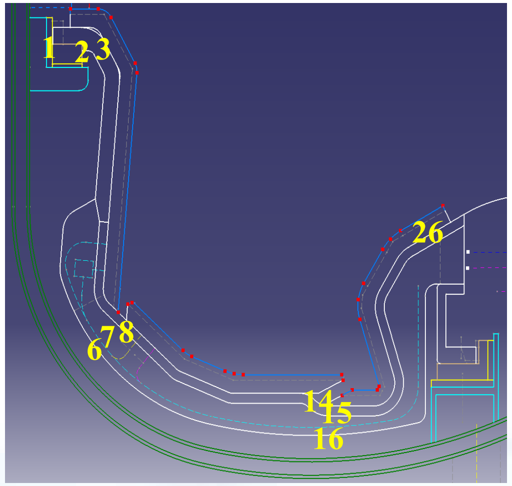

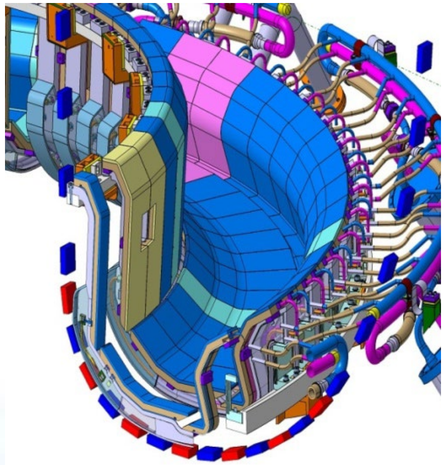

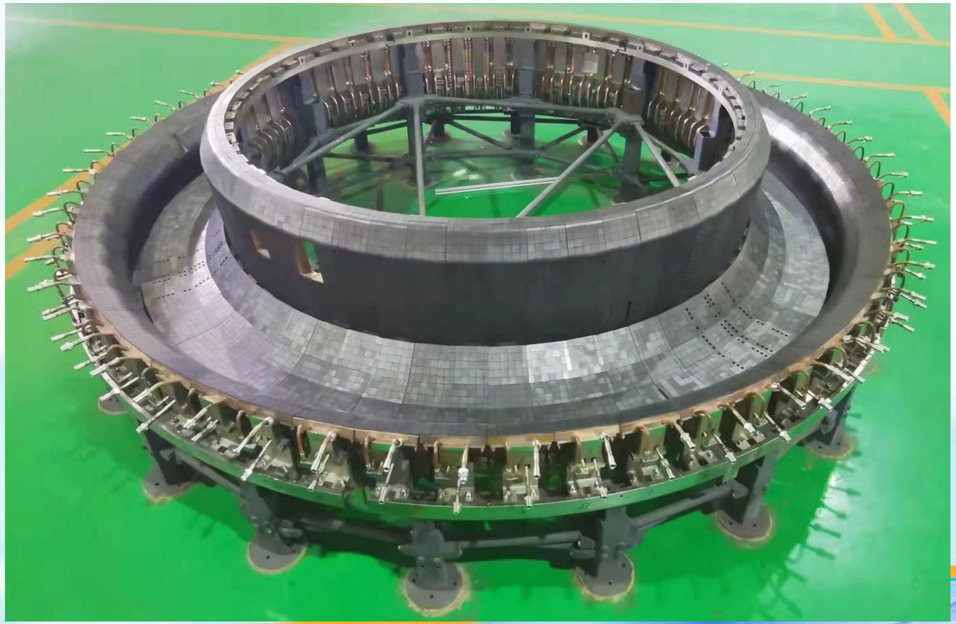

Hybrid and Steady state scenarios

- Hybrid scenario can be realized with Ip=1.0~1.4MA, f_G~0.5, the fractions of bootstrap current f_{BS} and total non-inductive current f_{ni} are between 30%~45% and 70%~90%, respectively
- Steady state scenarios, such as the hybrid steady state regime and the regime with a reversed magnetic shear, could be reached around 1MA of plasma current with f_{BS}>50% , H_{98}(y,2)~1.3

Ip(MA)/ B_t(T)	1.4/2.2	1.0/2.0	1.0/2.0
κ/δ	1.8/0.5	1.8/0.5	1.8/0.5
a/R(m)	0.65/1.78	0.65/1.78	0.65/1.78
f_G	0.47	0.5	0.5
$P_{NBI}/P_{EC1}/P_{LH}$ (P_{EC2})	10 /5 /(2)	6 /7 /(1)	6 /6 /3
X_{EC}/X_{LH}	0.34 /(0.28)	0.4 /(0.2)	0.3 /0.7
q_{95}	5.5	4.8	4.7
q_0/ q_{min}	1.10 /0.80	1.10 /1.00	0.93 / 0.88
β_p	1.3	1.7	1.6
β_N/4li	2.3 /3.8	2.5 /3.9	2.4 /3.4
f_{BS} /f_{ni}	0.33 /0.76	0.40 /0.86	0.41 /0.89
Te0/Ti0 (keV)	8.4/9.2	6.7 /6.1	6.5 /5.8
Teped/Tiped (keV)	1.0 /0.87	1.2 /0.86	1.3 /0.89
neped/nesep (1e19)	3.9 /1.1	2.7 /1.1	2.5 /1.3
W_{th} (MJ)	1.3	0.85	0.82
H_{98}(y,2)	1.05	1.1	1.03

Ip(MA)/ B_t(T)	1.2/1.7	1.0/1.85
κ/δ	1.8/0.5	1.8/0.5
a/R(m)	0.65/1.78	0.65/1.78
f_G	0.5	0.73
$P_{NBI}/P_{EC1}/P_{LH}$	10 /5.5 /-	1.5 /3.5 /4
X_{EC}/X_{LH}	0.42 /-	0.45 /0.6
q_{95}	5.1	4.8
q_0/ q_{min}	1.0 /1.0	1.10 /1.00
β_p	1.8	1.9
β_N/4li	3.4 /4.0	2.3 /3.2
f_{BS} /f_{ni}	0.55 /1.00	0.63 /1.00
Te0/Ti0 (keV)	7.5/12.0	4.0 /4.0
Teped/Tiped (keV)	1.1 /0.79	0.57 /0.35
neped/nesep (1e19)	2.9 /0.93	3.0 /1.0
W_{th} (MJ)	1.3	0.95
H_{98}(y,2)	1.29	1.32

PUMP with Puff to screen impurity and control Z_{eff}

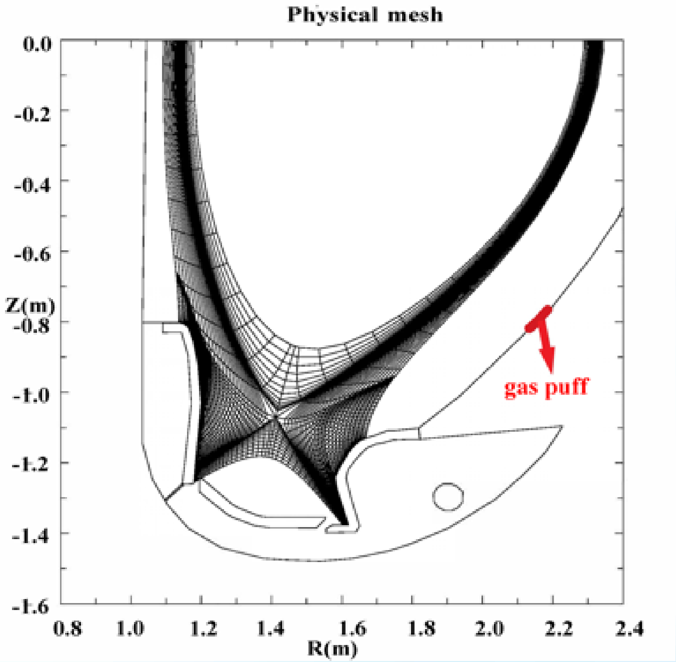

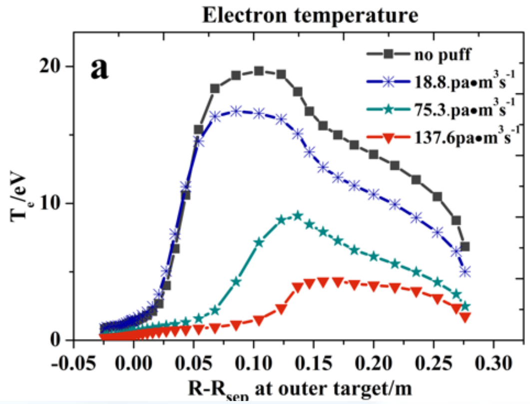

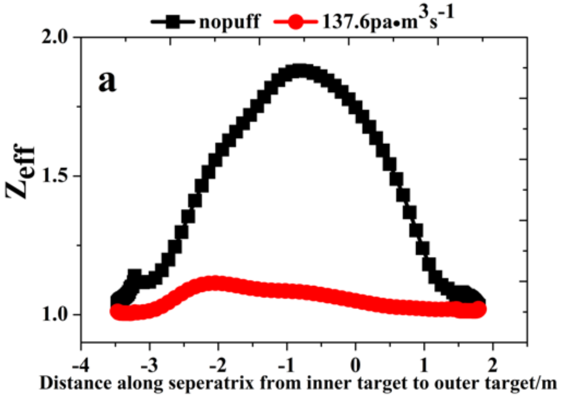

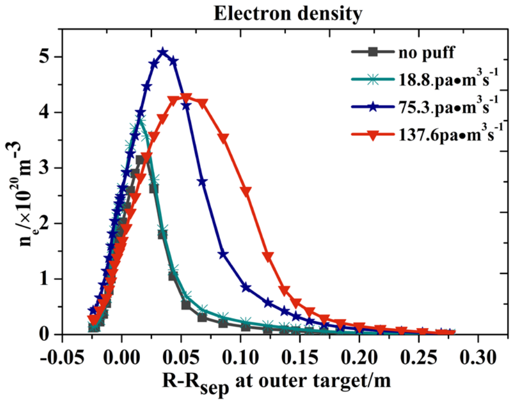

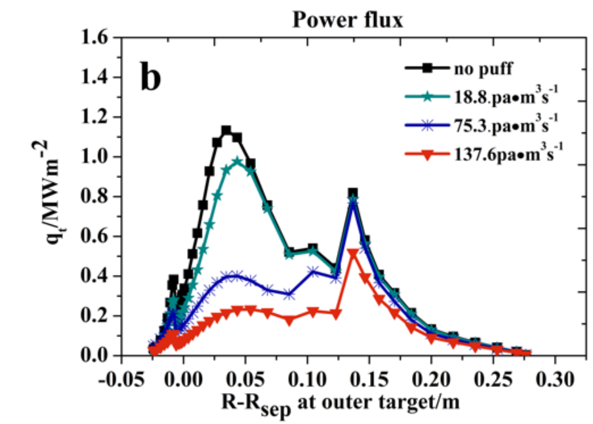

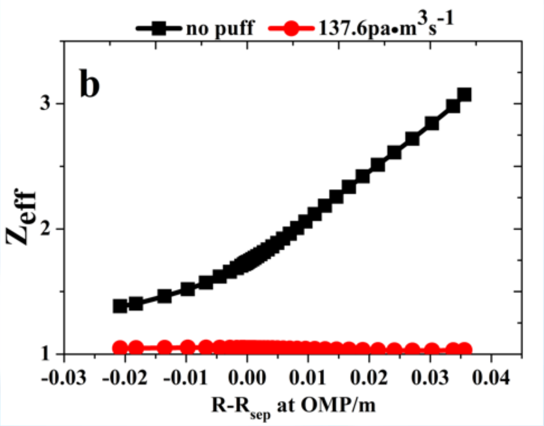

By combining the pump and puffing, Zeff can be reduced due to the strong viscous force acting on carbon impurity

Effect of drift HL-2M V Divertor

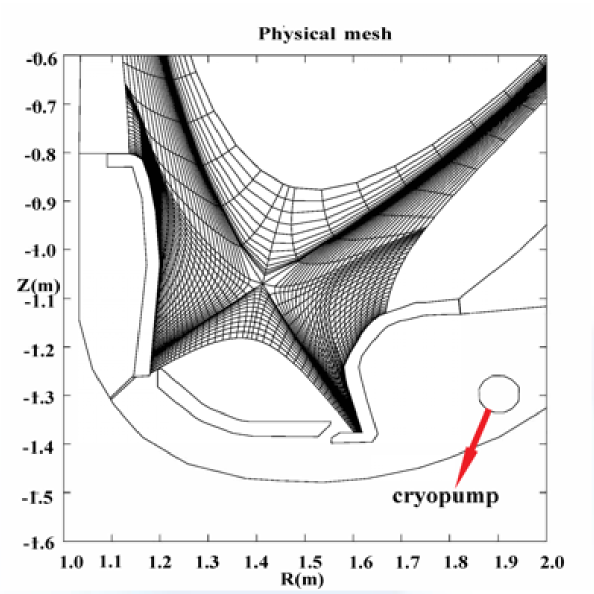

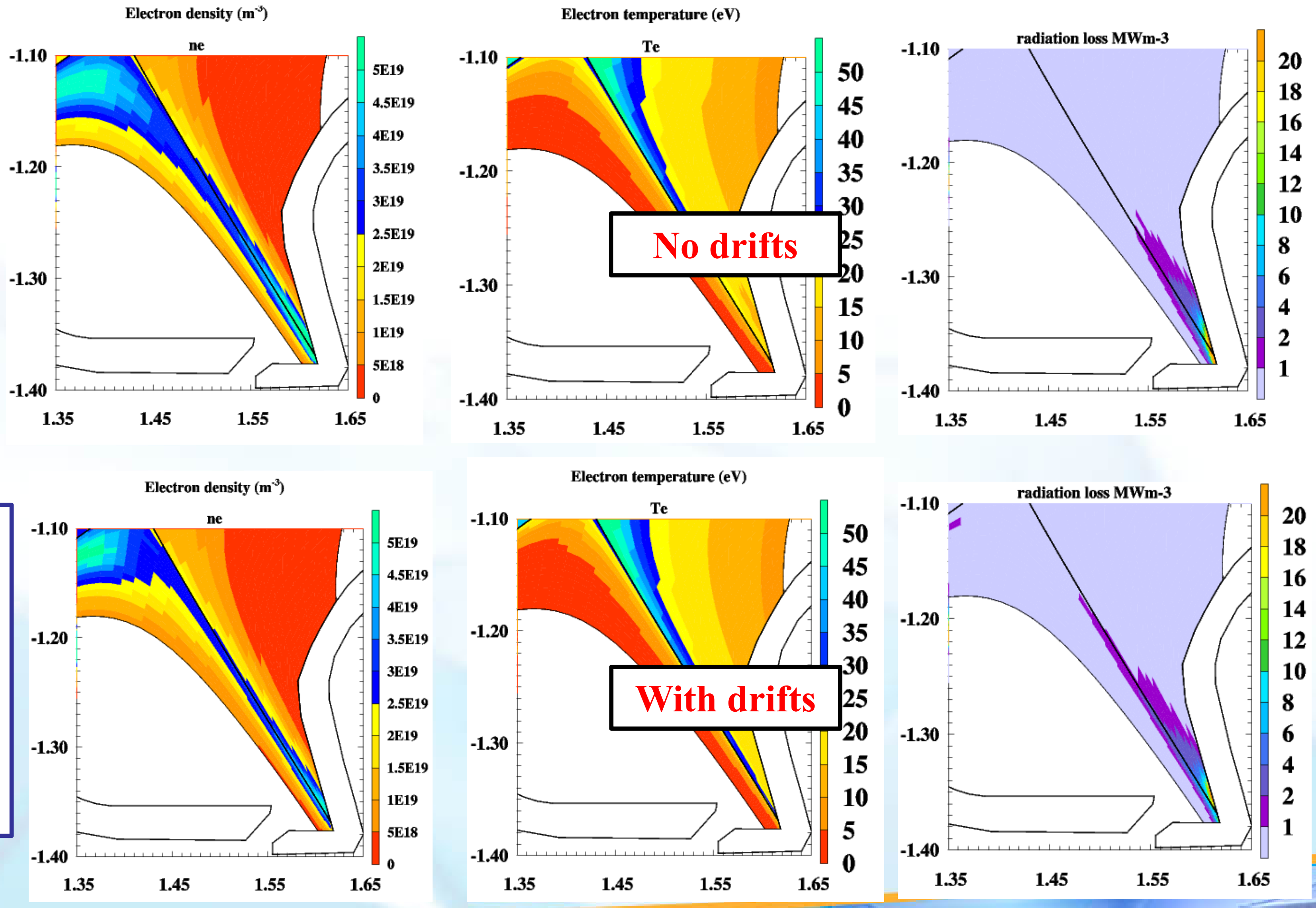

SOLPS modeling showed the drift have a relative small effect on HL-2M V Divertor due to the private flux region particle reflecting baffle. Due to the small drift effect, HL-2M V Divertor can better abstain detachment.

Controlling target Heat loading and Core *Zeff*

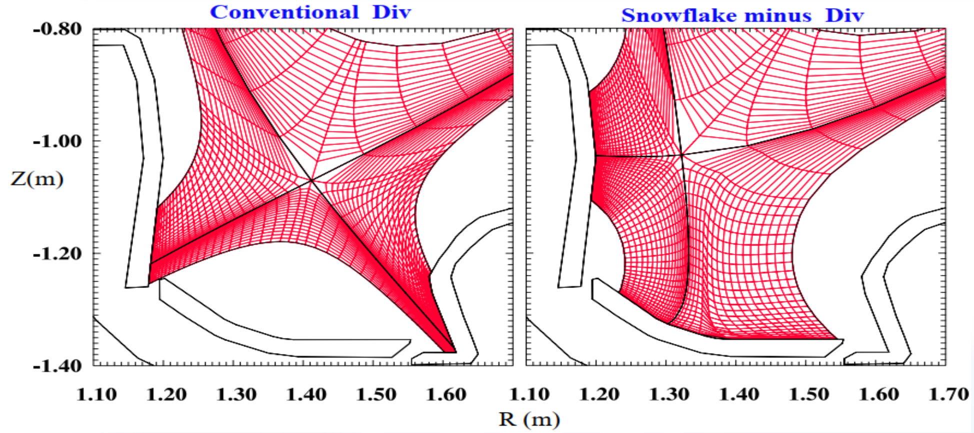

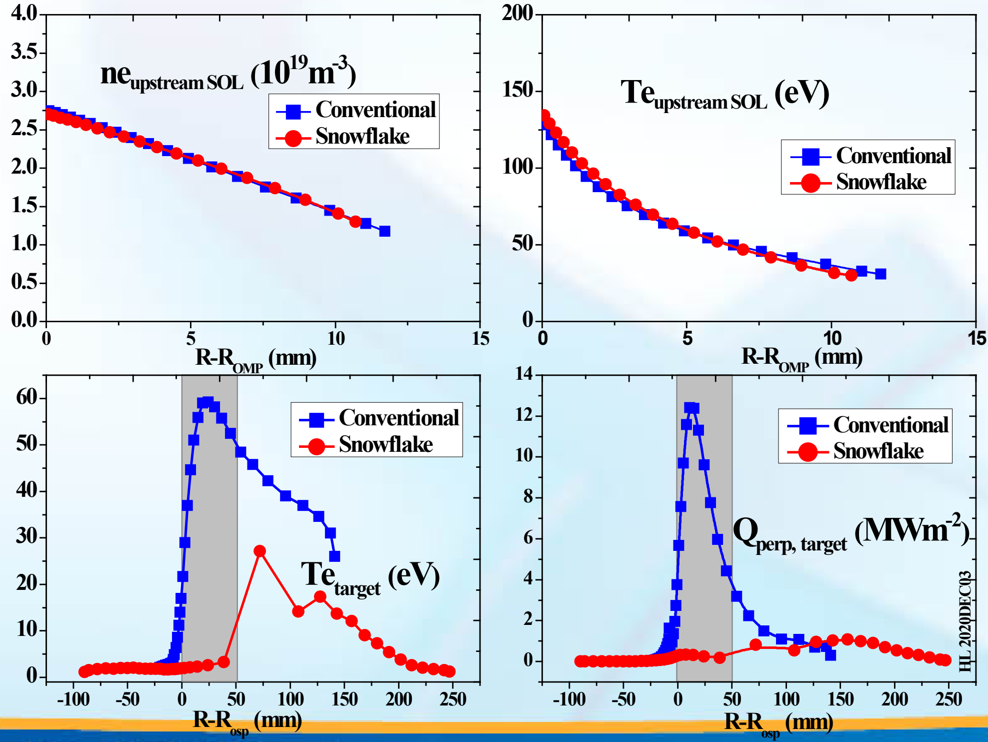

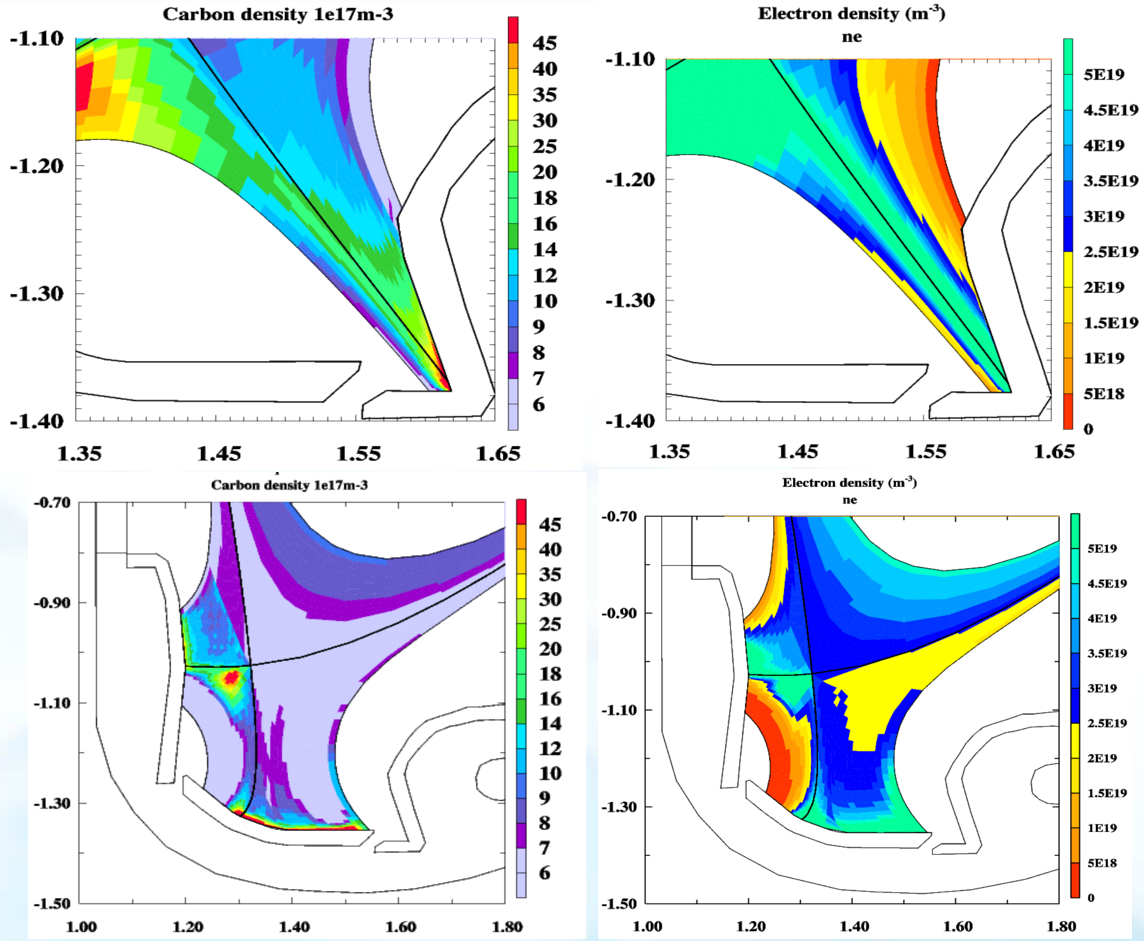

SOLPS modeling without drifts showed that the snowflake divertor can better screen recycling particles and carbon impurity than conventional divertor, so that the snowflake can better control heat loading and core effective Zeff than conventional V divertor.

E×B drifts effect on HL-2M SF- controlling target Heat loading

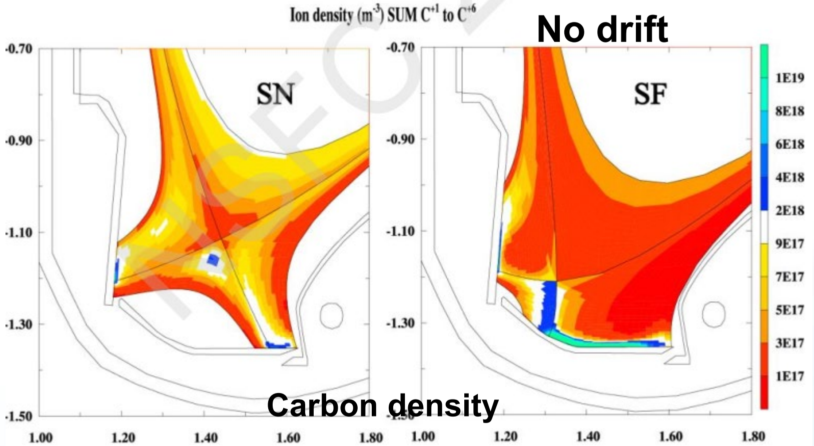

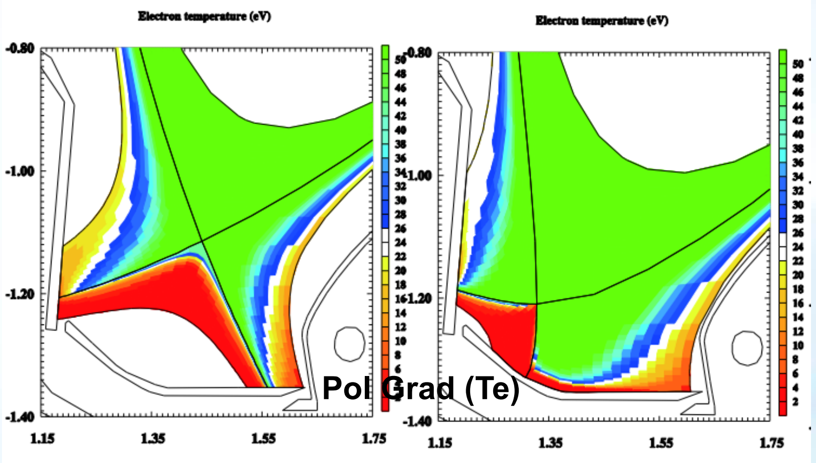

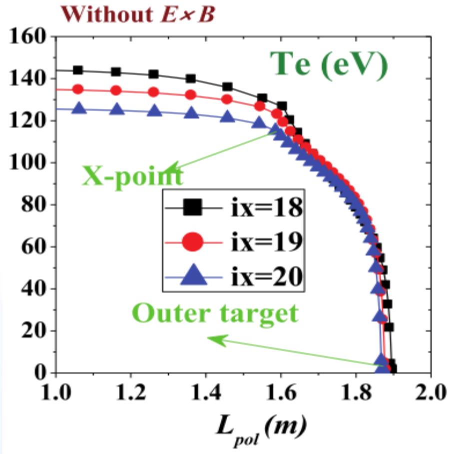

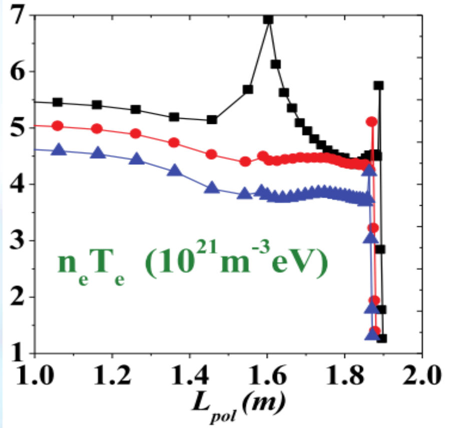

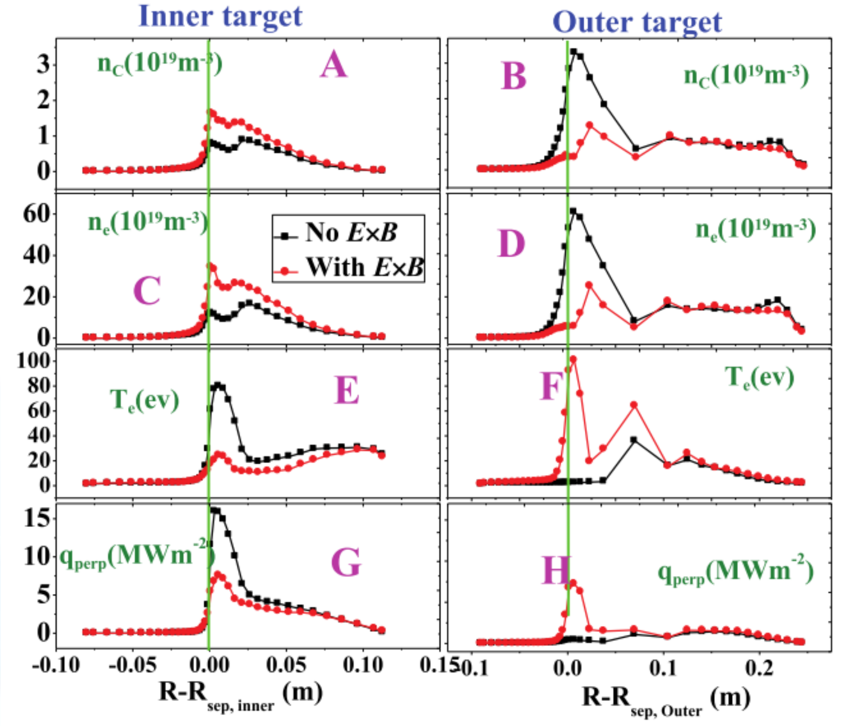

Fig. 2. The electron density n_e, C impurity density n_c, T_e and q_{perp} along the LITP and LOTP without/with $E \times B$, with **case2_mid** RATCs ($D_n = 0.3\ m^2/s$, $X_{e,i} = 1.0\ m^2/s$).

SF- can better screen recycling and carbon impurity particles than SN, so that the SF poloidal gradient Te is larger than SN.

The effect of drifts on SF is stronger than SN due to the stronger poloidal T_e gradient. Drift can push a lot of recycling particle and carbon impurity out of SF- region, so that the target heat loading can be enhanced greatly by drifts.

Impact of drifts on HL-2M SF- detachment Cliff by SOLPS

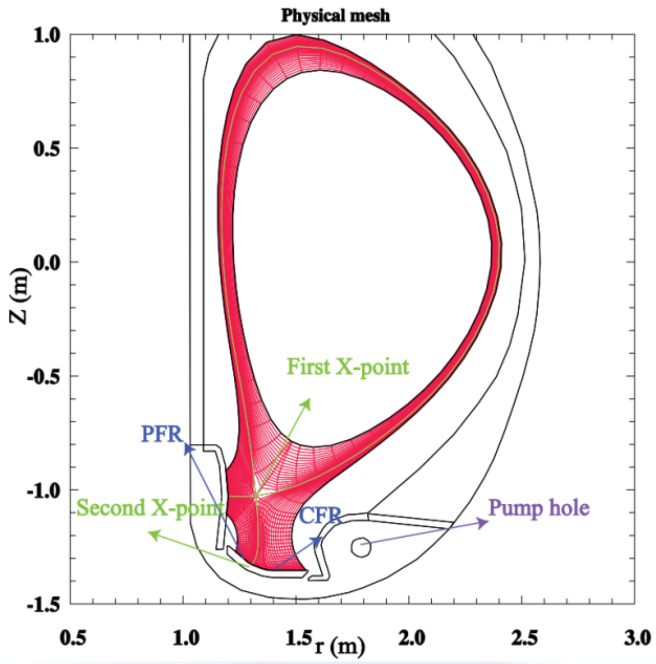

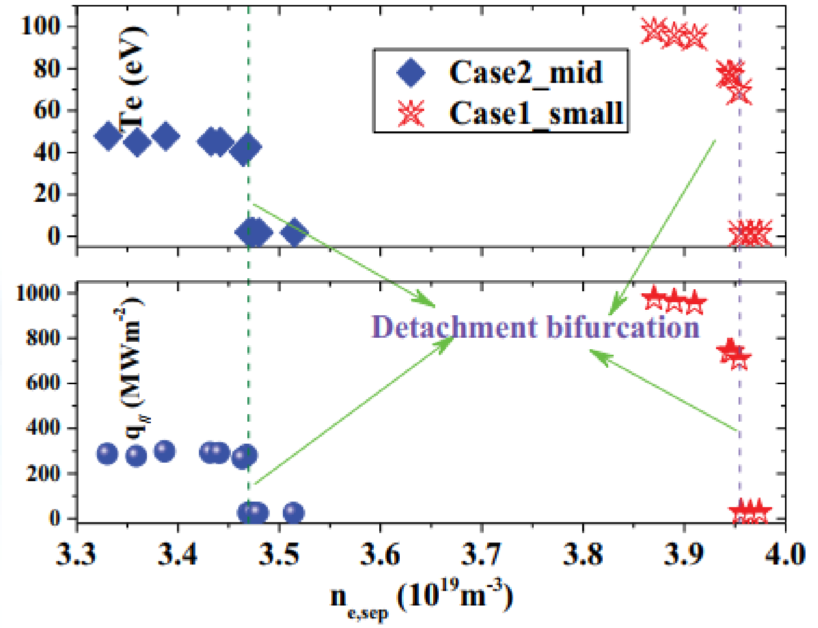

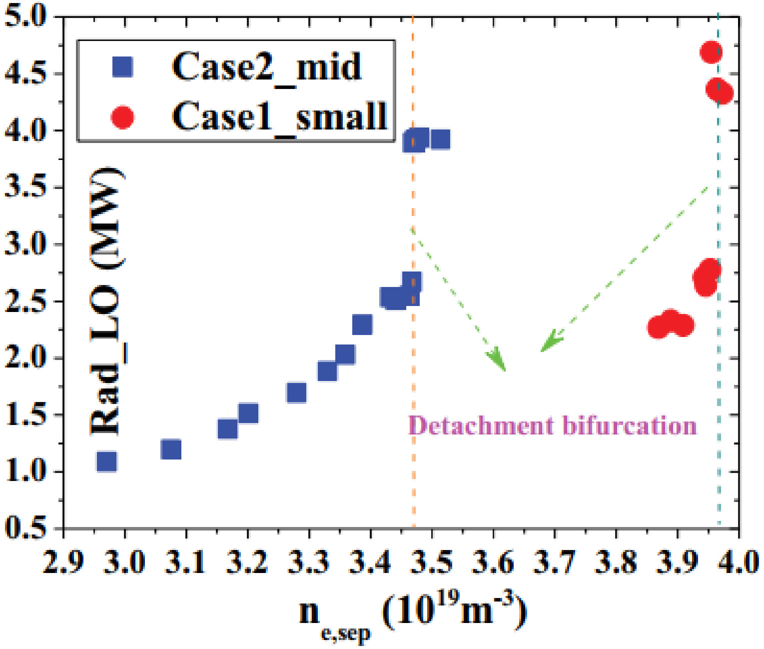

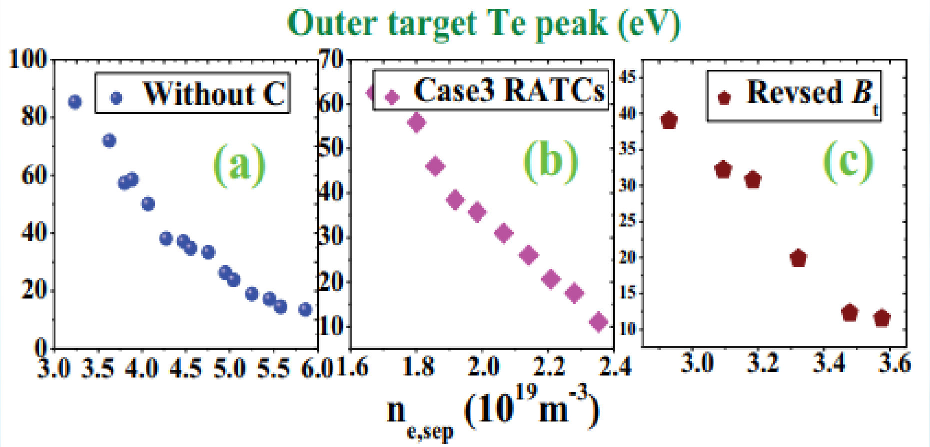

SOLPS modeling showed Detachment cliff also could appear for SF- under the given conditions, including: E× B drift, relative small radial transport, carbon impurity, Fav.Bt.

The interaction between E× B, radial grad(T_e),and radiation loss is the root reason for detachment cliff.

H. L. Du, Nuclear Materials and Energy, **22**, 100719 (**2020**).

Impact of drifts on DIII-D detachment Cliff by SOLPS

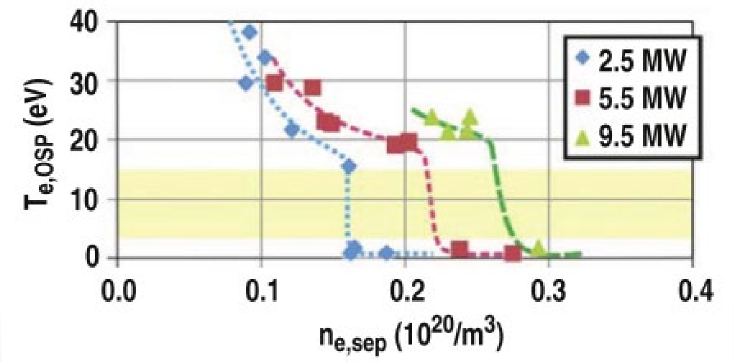

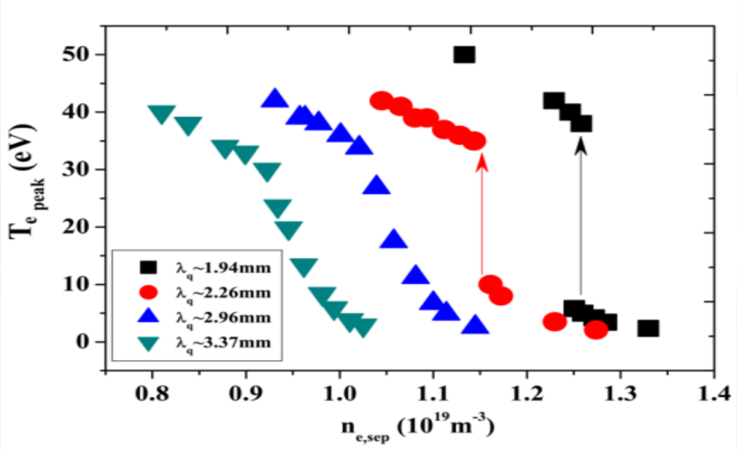

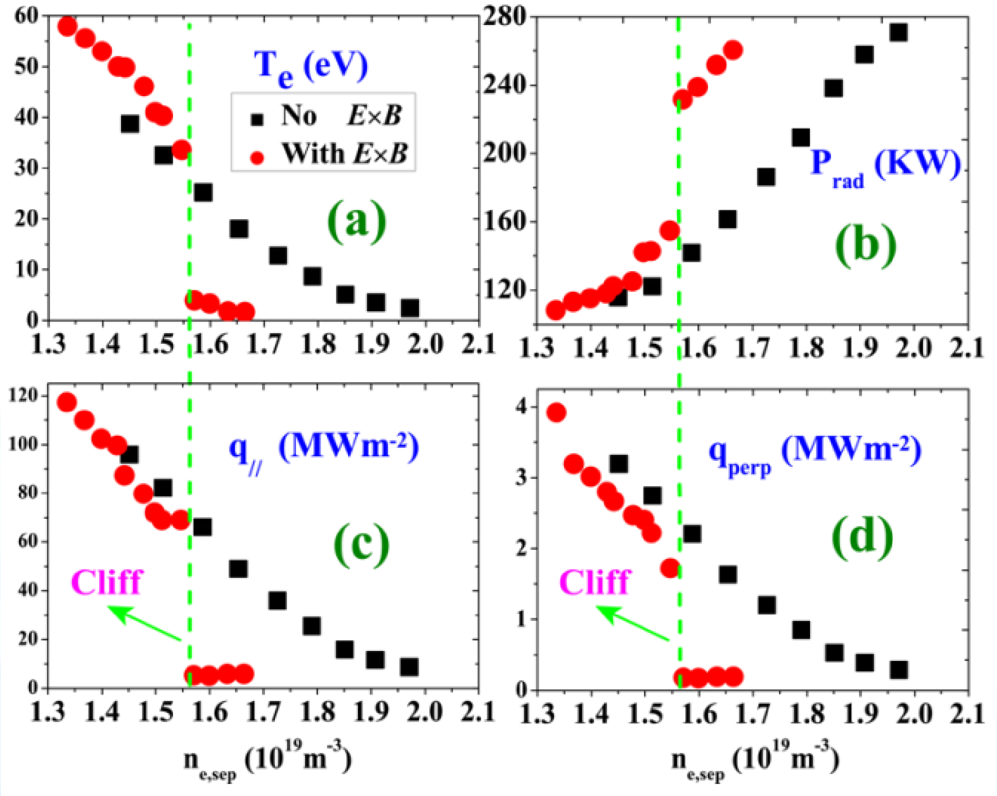

By modeling, we found Cliff necessary conditions and its produced root reason. The necessary conditions including: E× B drift, relative small radial transport, carbon impurity, Fav.Bt .

SOLPS with E× B drift can well reproduce the experimental Detachment cliff results, and showed the E× B drift is a necessary condition of detachment cliff.

Neutral particles in Favorable-Bt with drifts

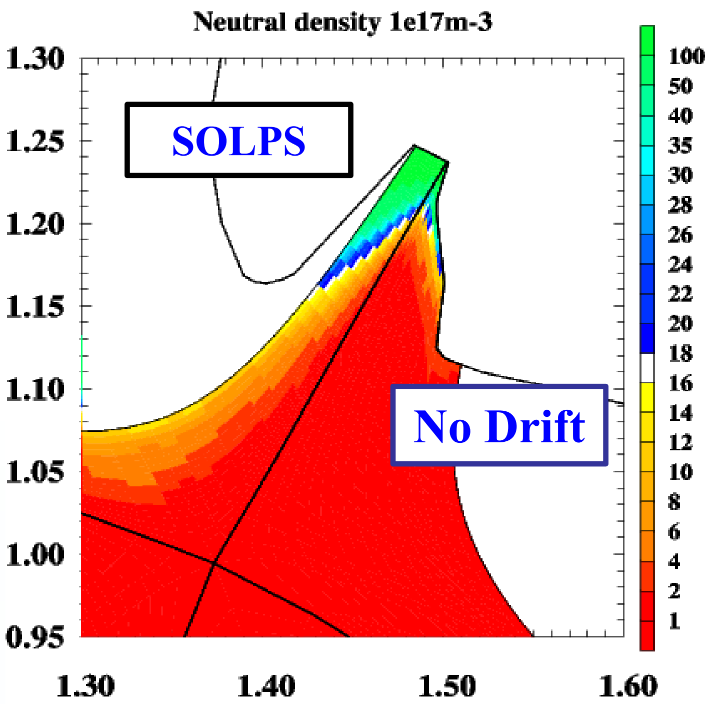

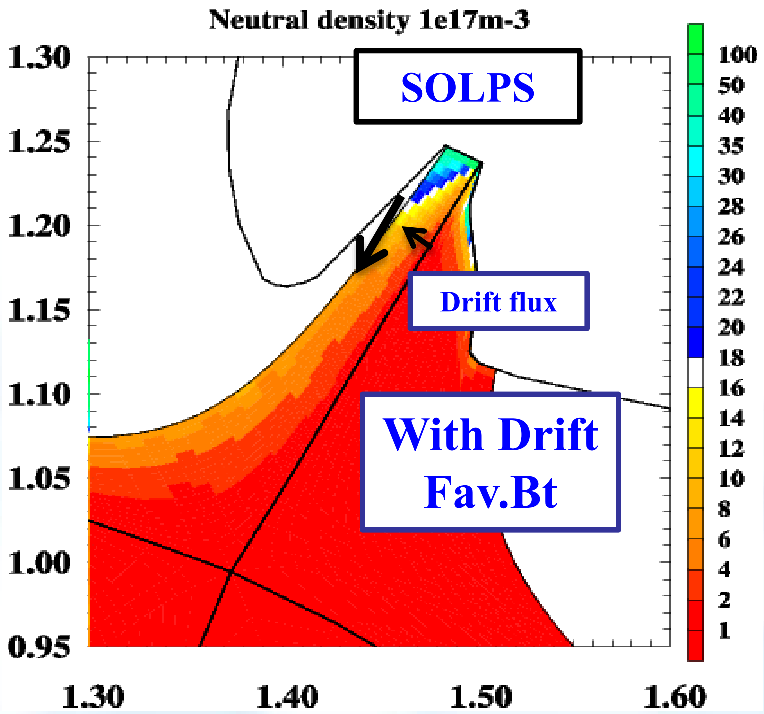

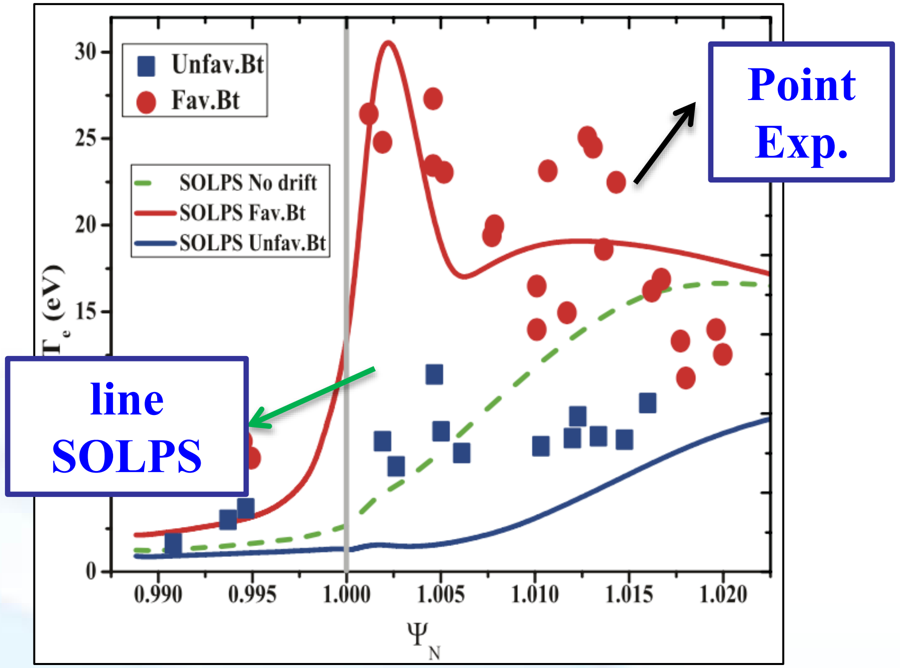

By SOLPS numerical modeling, we find that E× B drift have very strong effect on SAS detachment. E× B drift can push a lot of particles out of SAS region, and almost offset the SAS trapping neutral particle capacity.

Reflecting baffle in PFR region reducing E×B flux

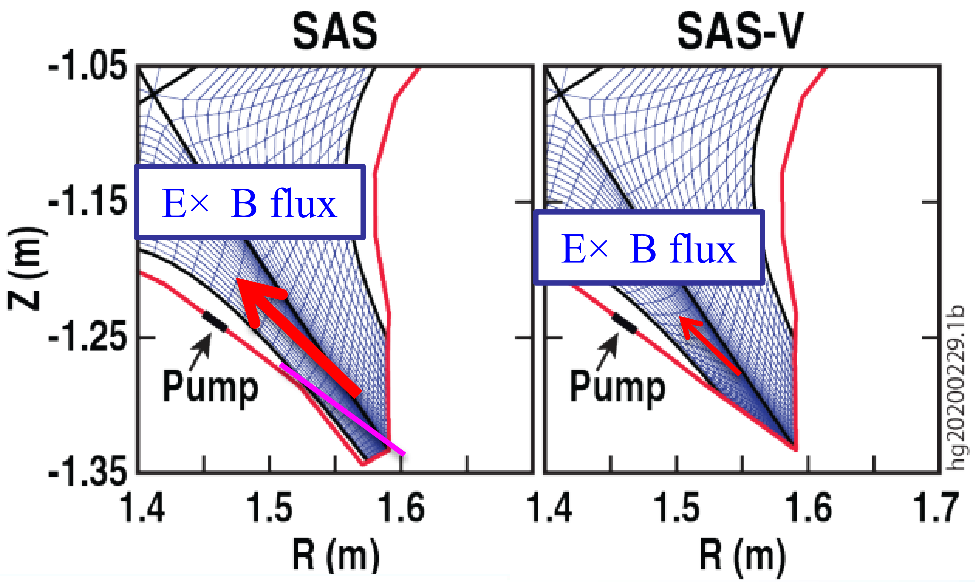

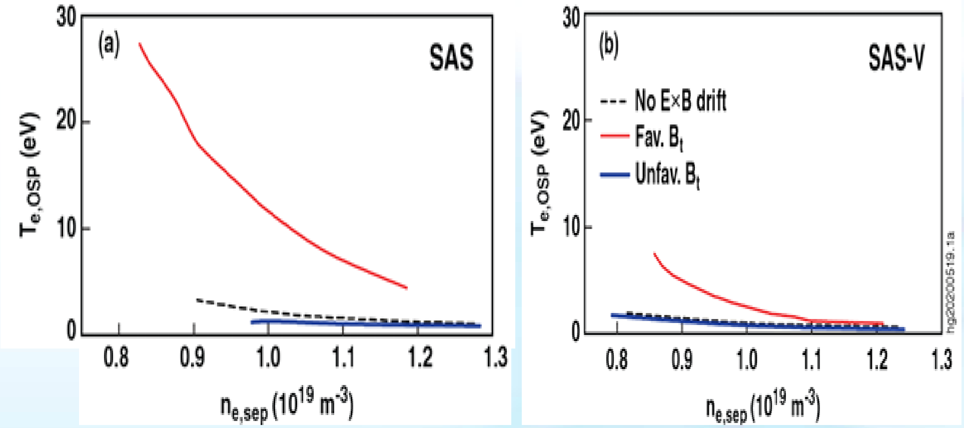

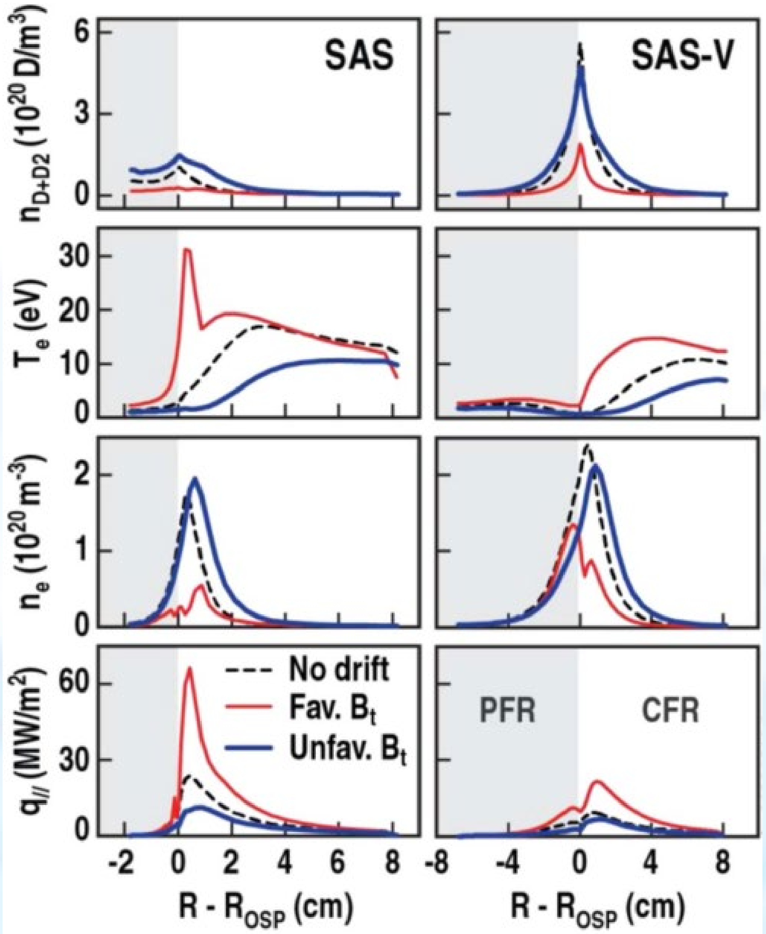

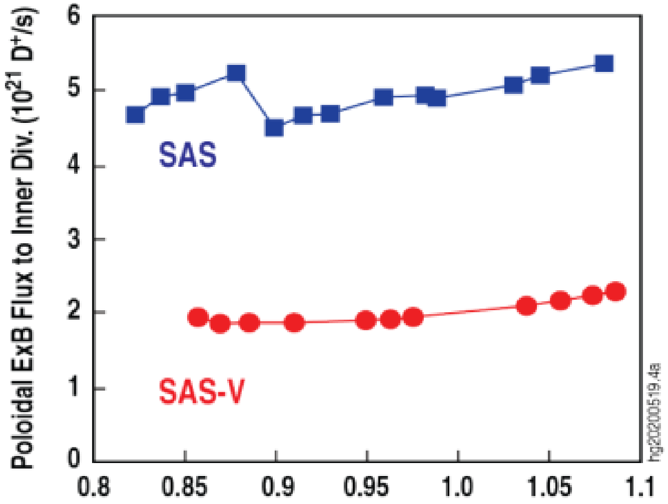

SOLPS-ITER showed that the E× B drift effect on detachment can be mitigated by adding a extra reflecting baffle in PFR region. As a result, the detachment can be achieved easily with relative low upstream density.

H.L. Du, H.Y. Guo, et al. Nucl. Fusion 60 (2020) 126030

HL-2M Plasma Control System

■ Consulting and control design support for deployment of HL-2M PCS

- 1 ms & 100 us control cycle with RT-linux being the operating system;
- Communication delay time ≤ 200 us with RFM
- Multi CPU and GPU, with strong capability of extension

Department of Energy
Washington, DC 20585

June 4, 2019

Dr. Tony Taylor
Vice President, Magnetic Fusion
Energy Division of General Atomics

Dear Dr. Taylor,

Given the anticipated benefit to the DIII-D National Fusion Program and the Department of Energy, I approve your request for the General Atomics Fusion Energy Division to provide to the Southwestern Institute of Physics (SWIP), in Chengdu, China the following software, which is described in detail in your pair of request letters dated June 3, 2019:

- An adaptation of the EAST/DIII-D PCS to operate the HL-2M tokamak, which includes:
  1. EAST/DIII-D PCS core plasma control "operating system" (infrastructure) code;
  2. EAST/DIII-D control algorithms intended to be executed by the PCS;
  3. EAST/DIII-D realtime EFIT algorithm; and,
  4. Machine and plasma emulation code for EAST/DIII-D, intended to be executed with Matlab/Simulink software and in Simserver mode with the HL-2M PCS software itself.
- The GA Tokamak System Toolbox (TokSys), which includes:
  1. Basic infrastructure scripts and functions for doing fundamental electromagnetic and plasma control analysis;
  2. Control design and simulation tools specific to HL-2M;
  3. Data objects and data handling codes specific to HL-2M; and,
  4. Controller definitions and simulation results specific to HL-2M.

If the terms of the GA/SWIP collaboration change, please notify me immediately.

Sincerely,

Dr. Matthew J. Lanctot
Program Manager - Advanced Tokamak and Long Pulse Tokamak
Fusion Energy Sciences
Office of Science
U.S. Department of Energy

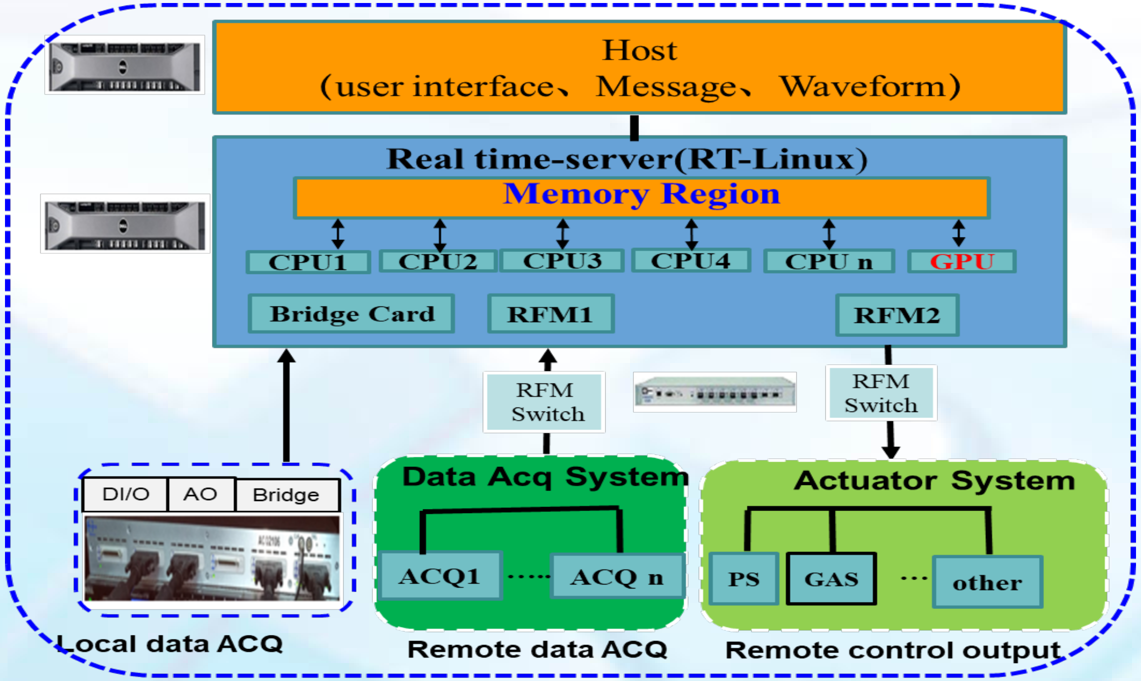

HL-2M PCS structure

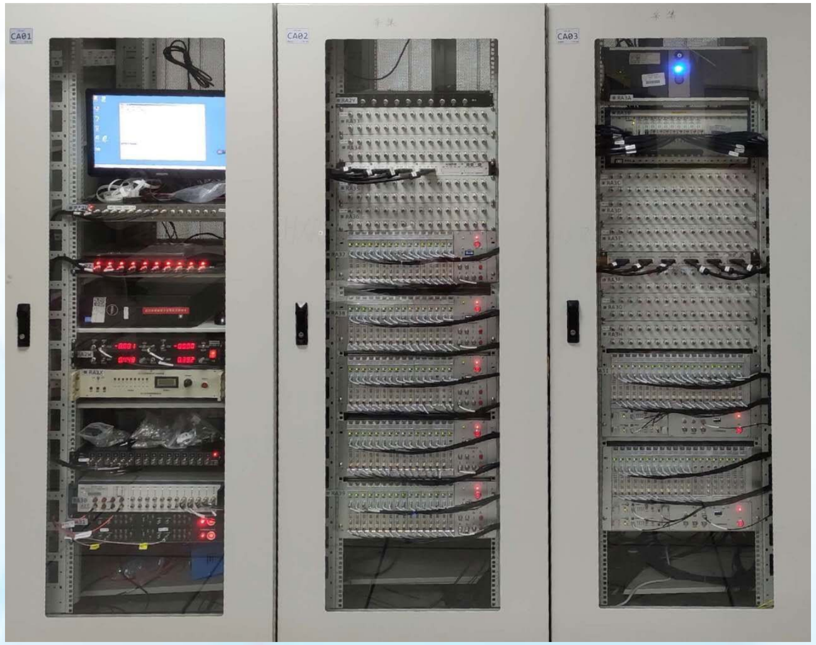

DAQ with 256 channel

Plasma equilibrium and Discharge Tools

Plasma equilibrium and discharge waveform design tools was developed with flexible user interface, successfully validated in HL-2M 1st plasma

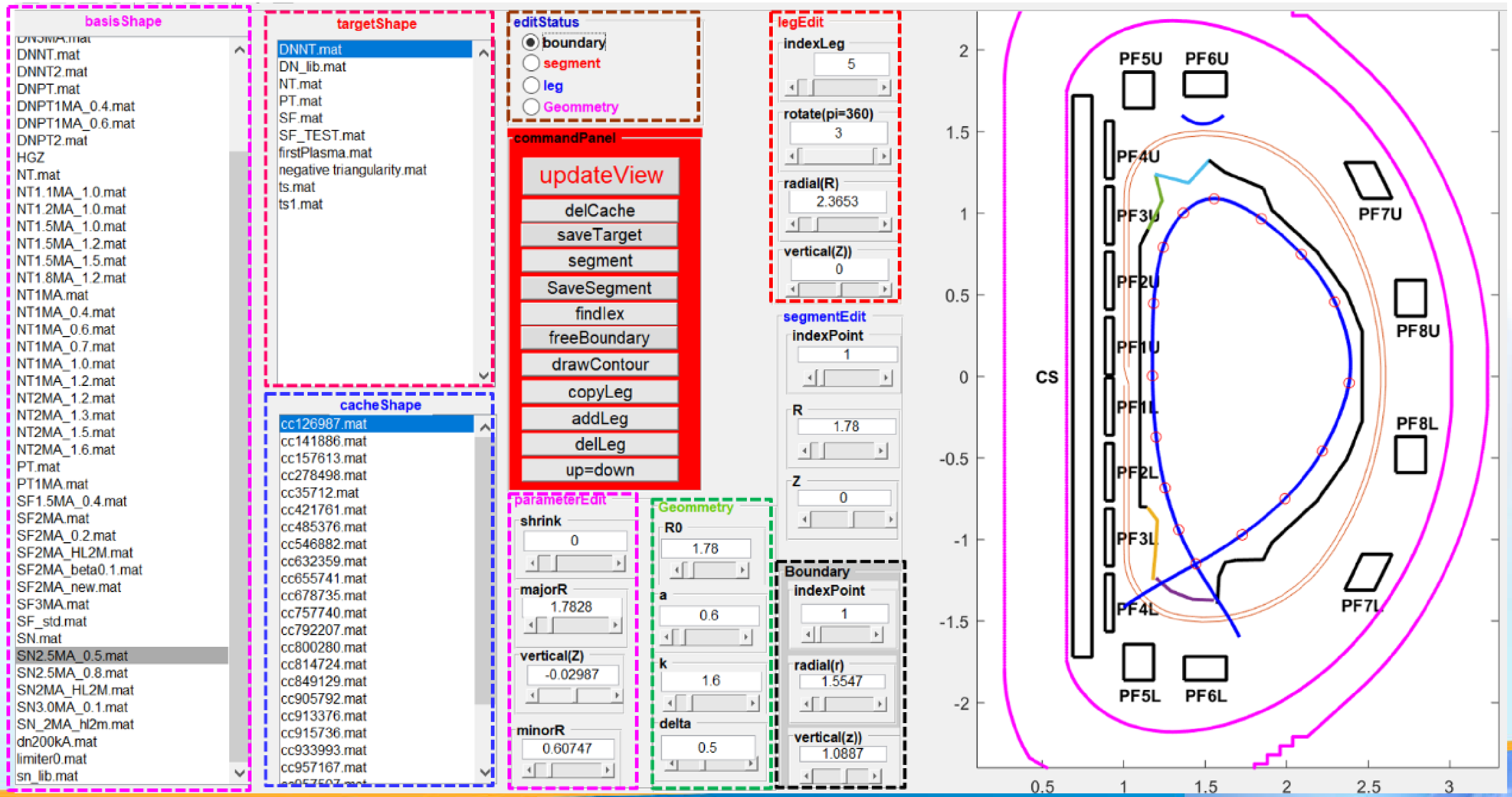

Fast Approach to Equilibrium design Tools

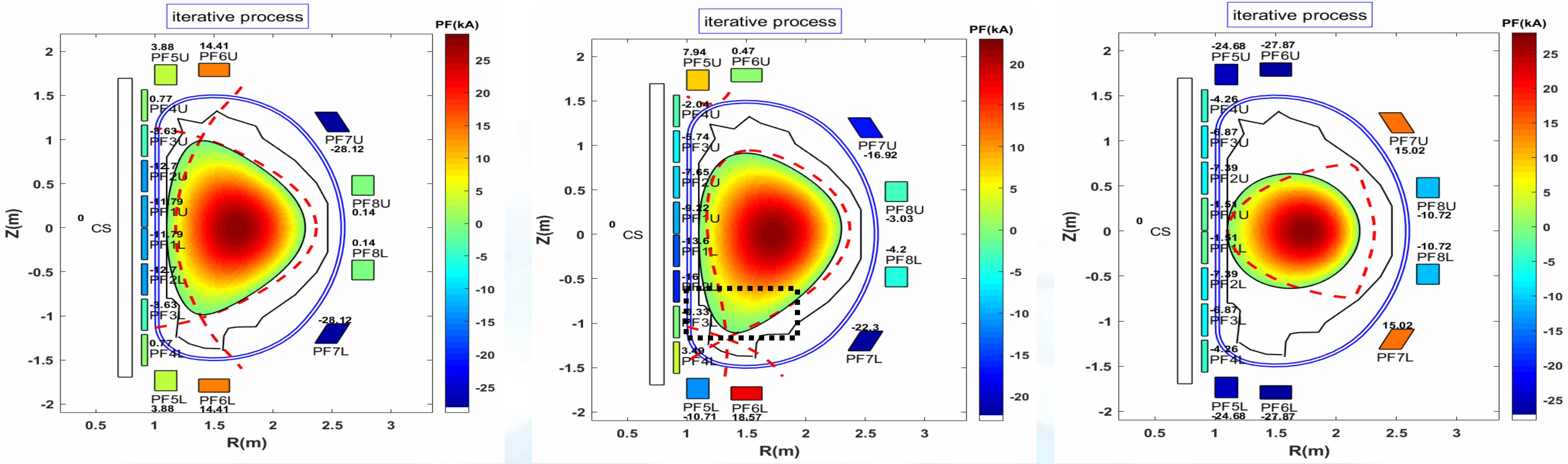

Step 1: given the desired target plasma shape by using the flexible user interface

Step 2: preset plasma and current distribution parameters

Step 3: select the PF coils used in plasma shaping

Step 4: set control weight for boundary , divertor leg and coil current

Feedforward Discharge Waveform Design Tools

- PF coil current is consisted of flux component (Ip control) and equilibrium component (shape and position control)
- Flux component□ plasma inductance & resistance consumption
- Equilibrium component is proportional to Ip

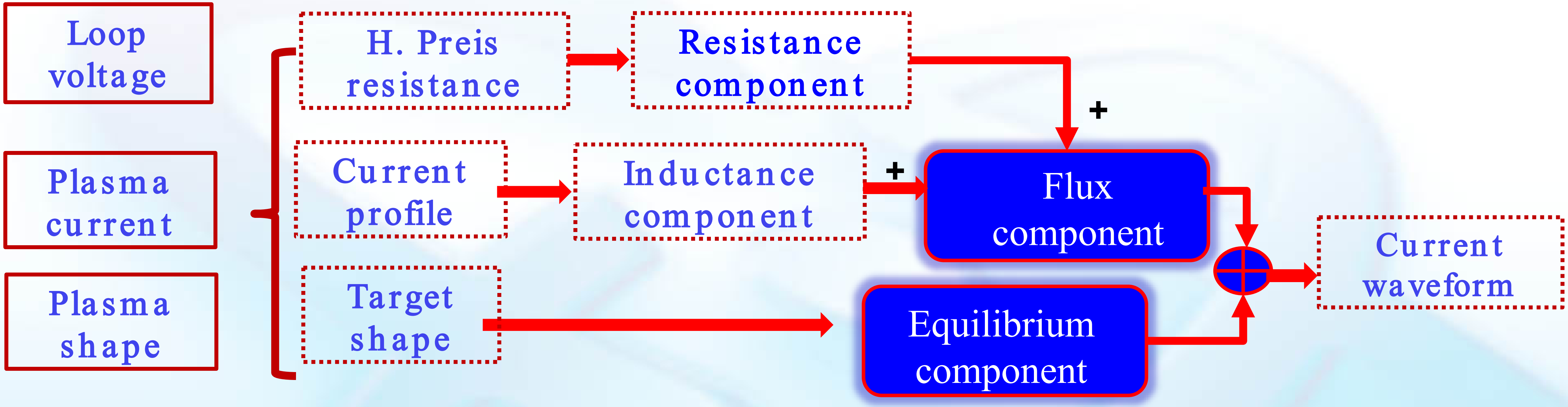

Plasma equilibrium and Discharge Tools

Plasma discharge waveform for limiter configuration with CS+PF6+PF8

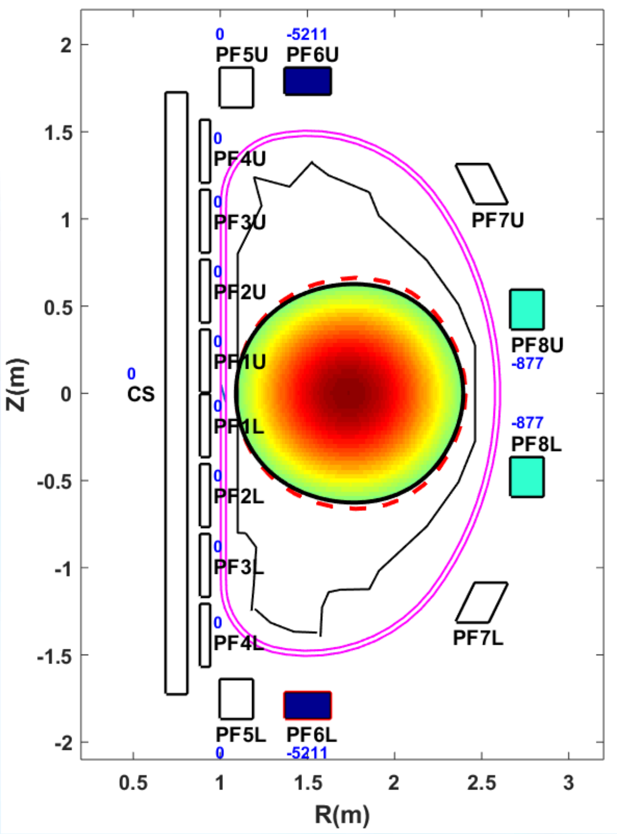

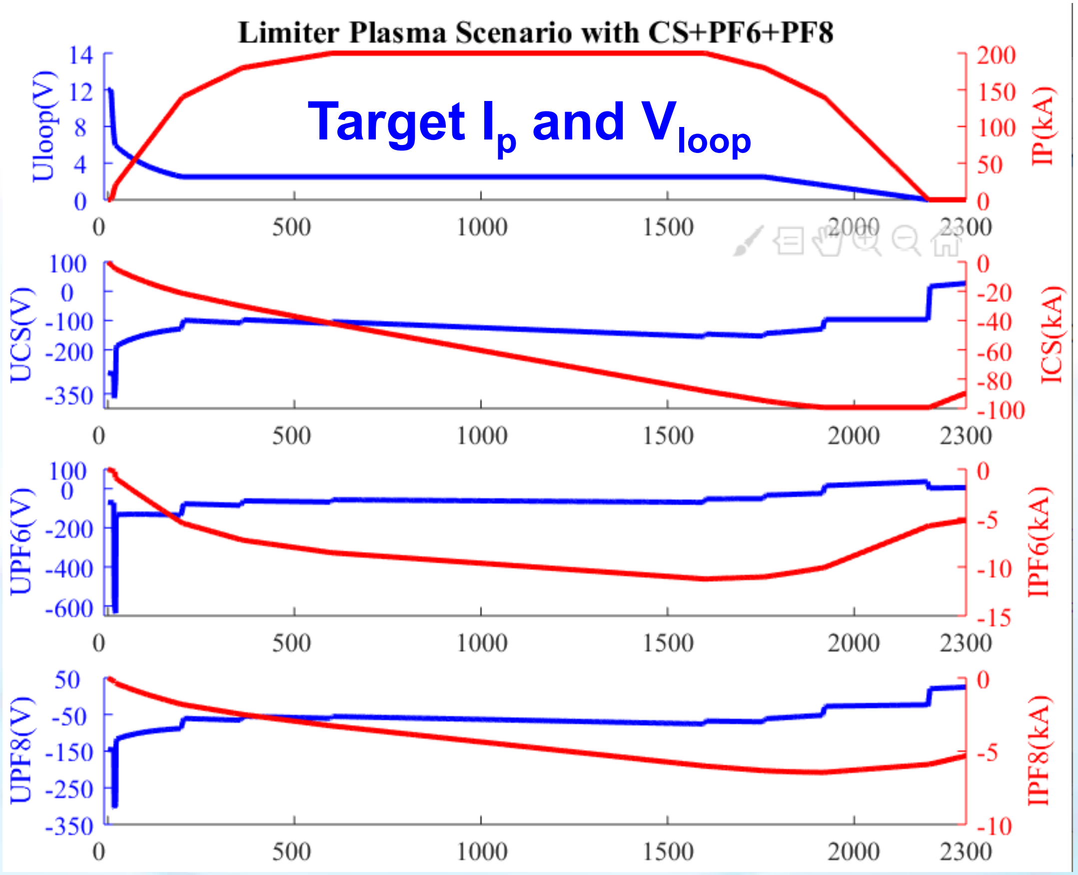

Has been successfully validated in HL-2M 1st plasma

HL-2M Hybrid mode scenarios design

SF Configuration evolution

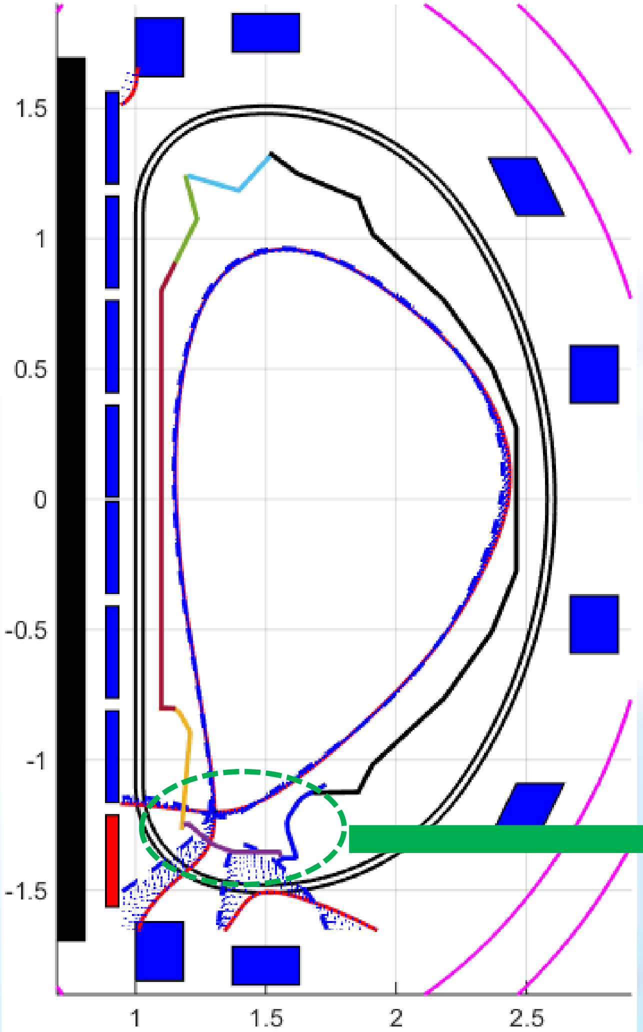

Hybrid mode scenarios by using OMFIT

To control the position of the X-point and the striking point are necessary.

The strike point and the second X-point change with the PF current

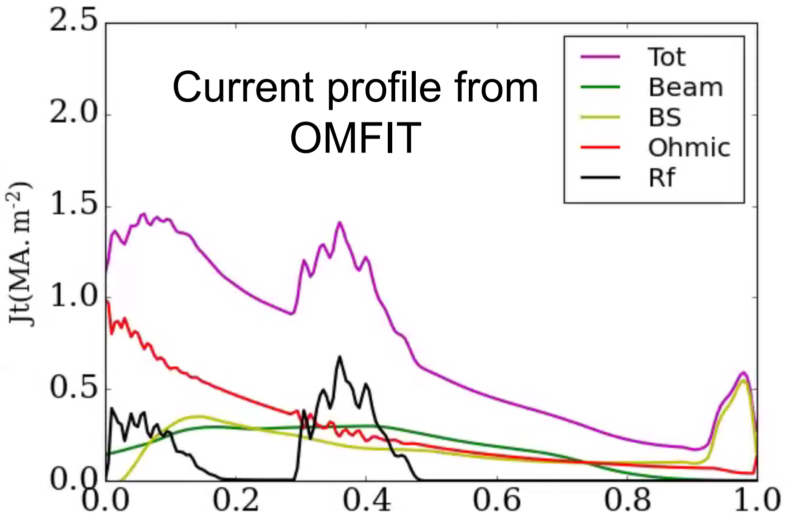

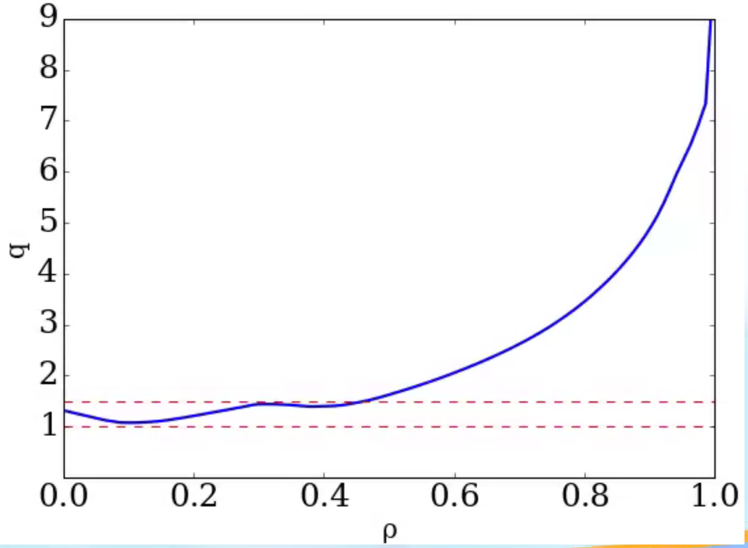

Advanced divertor configuration control

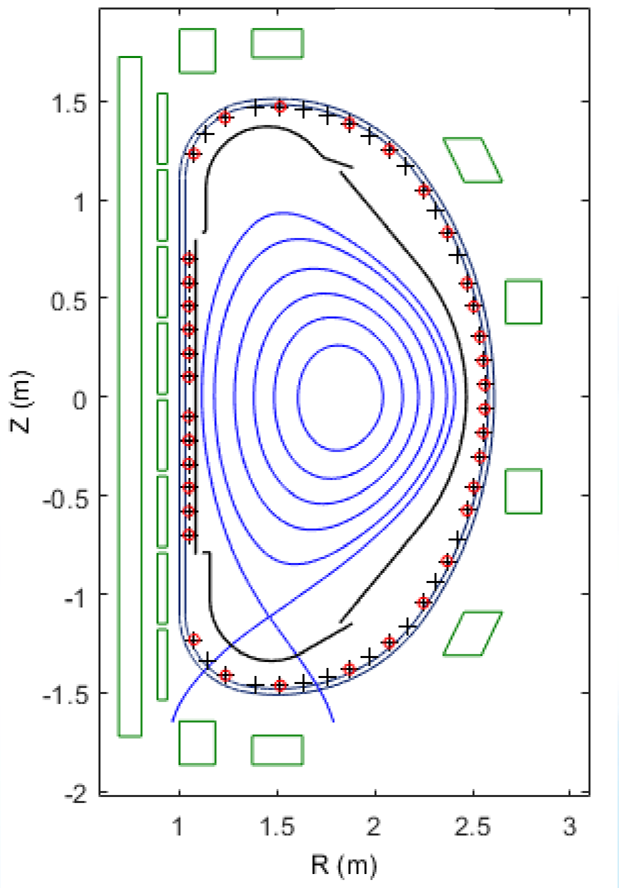

Magnetic probe layout for configuration reconstruction

- **Magnetic probes: 50 × 4 arrays 2-D (pol.&tor.)**
  - RTEFIT
  - Boundary and X-point reconstruction technique
  - Advanced divertor control algorithm

- **Optical plasma boundary reconstruction for plasma position control**
  - Localized light emission from the plasma boundary in tangential view, visible images results in clearly resolved boundary edge-features.
  - High temperature on the target surface for the strike point with IR camera

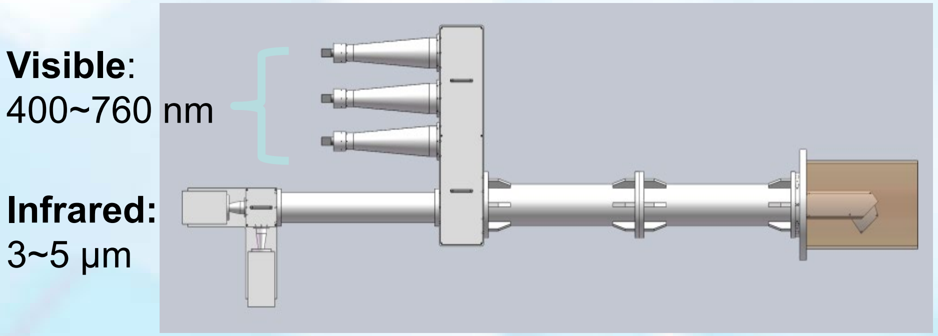

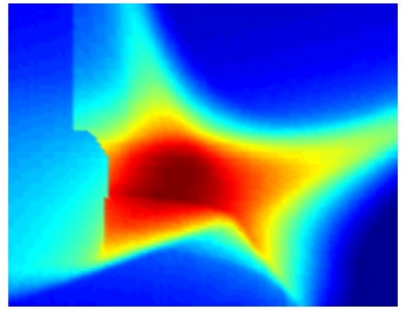

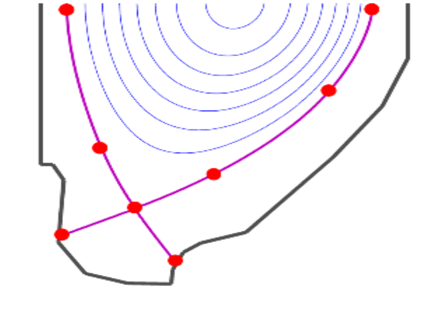

Advanced Divertor Control Algorithm

- Locally expand the Grad-Shafranov equation:

$$r\frac{\partial}{\partial r}\left(\frac{\partial \psi}{r\partial r}\right)+\frac{\partial^2\psi}{\partial z^2}=0 \Longrightarrow \psi_{\exp}=\psi(C_{\exp},x,y)$$

- Find coefficients, C_{exp}, with the Br and Bz at points(P0-P3) from RTEFIT

- Created the relationship between the PF coils current and the X-point locations:

$$\frac{\partial \delta x1}{\partial \delta I_{PF}}=\frac{\partial \delta x1}{\partial C_{\exp}}\left(\frac{\partial C_{\exp}}{\partial B_r}\frac{\partial B_r}{\partial \delta I_{PF}}+\frac{\partial C_{\exp}}{\partial B_z}\frac{\partial B_z}{\partial \delta I_{PF}}\right)$$

→ **X, P , G**

- Consider the configuration control

$$\delta I_{PF}=(A^T A)^{-1}\cdot A^T\cdot W\cdot B$$

where, $A=\begin{bmatrix} G_{iso} \\ X\cdot P\cdot G \end{bmatrix}$

$B=[\delta\psi_{iso},\delta x_1,\delta y_1,\delta x_2,\delta y_2]^T$

Control X1, X2, ρ, θ

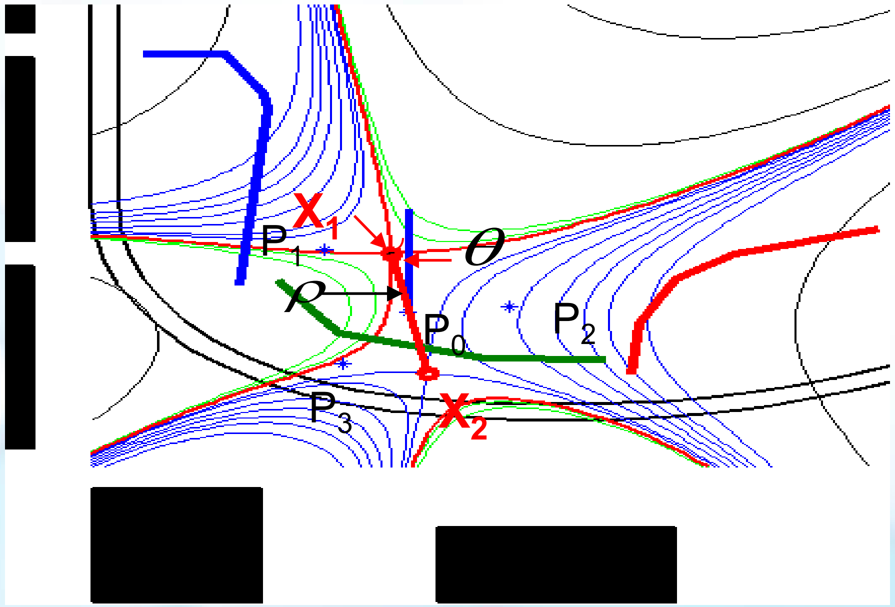

Advanced Divertor X Point Control Simulation

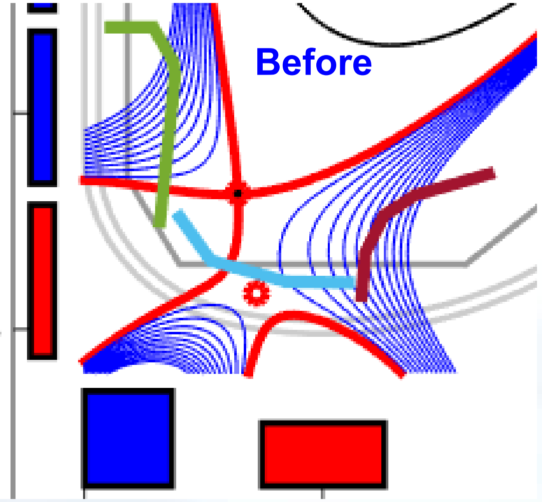

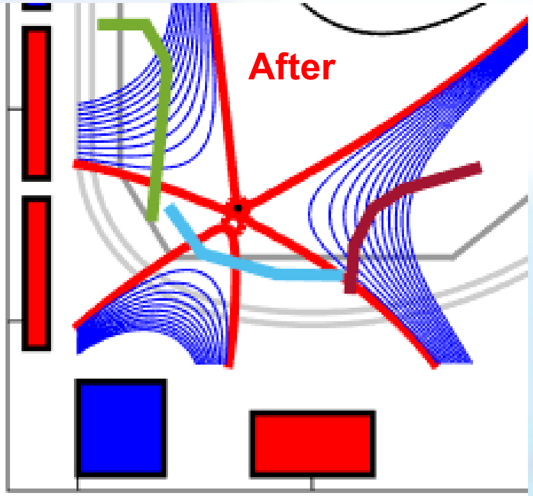

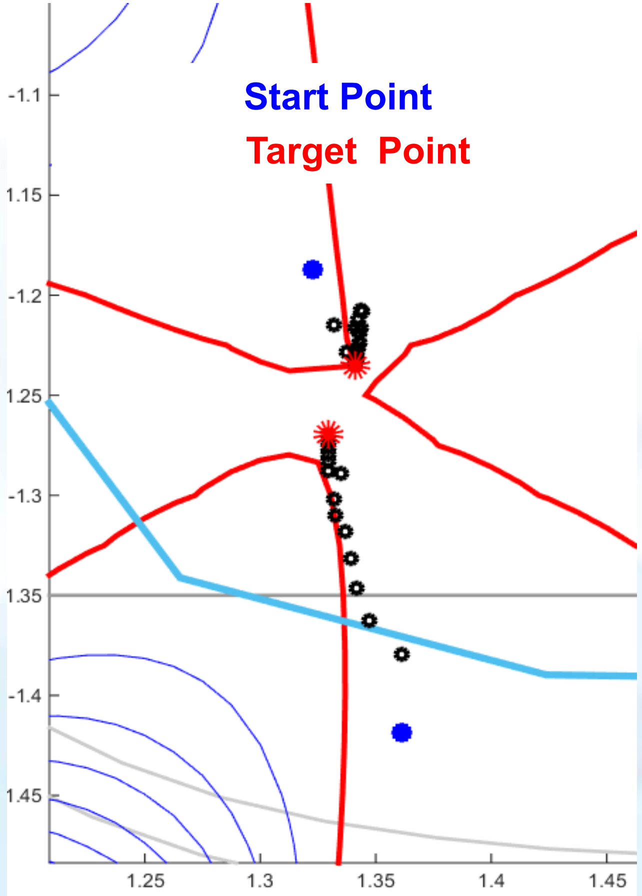

X Point motion in control

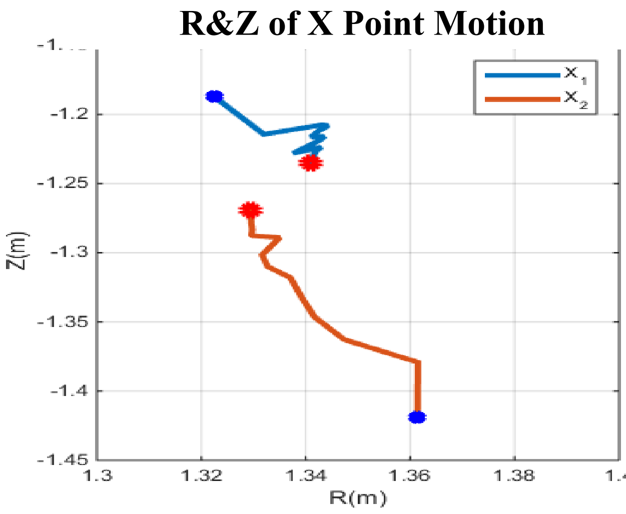

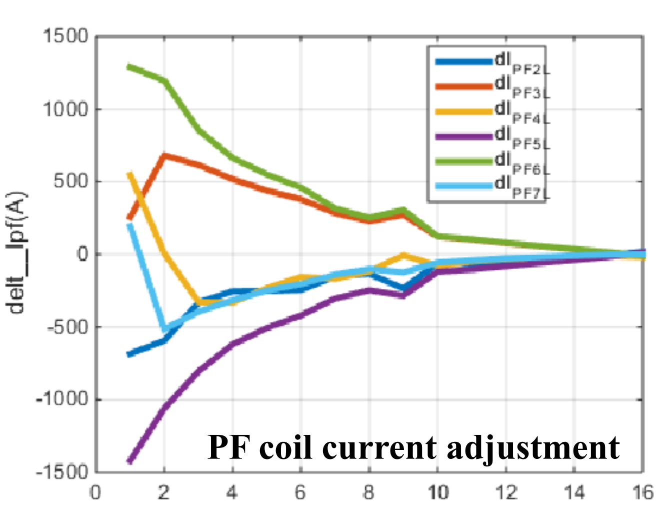

Divertor Detachment Feedback Control Platform

- Platform structure, including simulation unit, feedback unit and condition unit, is designed in RT-LINUX.
- Flexible combination of 4 SMBI systems is designed for the detachment control, referring SOLPS simulation result.
- SMBI Parameters： 10^{18}~10^{23}/s, (D^2, Ar, N, Ne, …, *etc.*)
- 172 groups of Langmuir probes are designed for the heat flux diagnostic (scope: 0.1~Several 100 eV)
- Simulation test injecting D^2 is performed, the of the strike point is mitigated significantly.

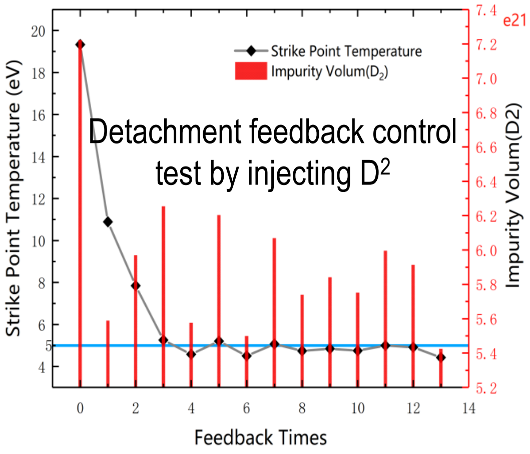

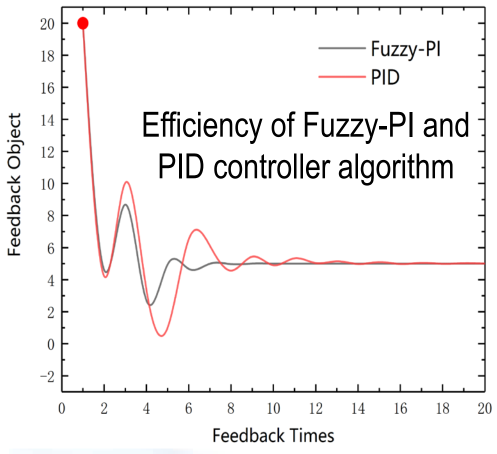

Langmuir probes designed for the real-time heat flux diagnostic

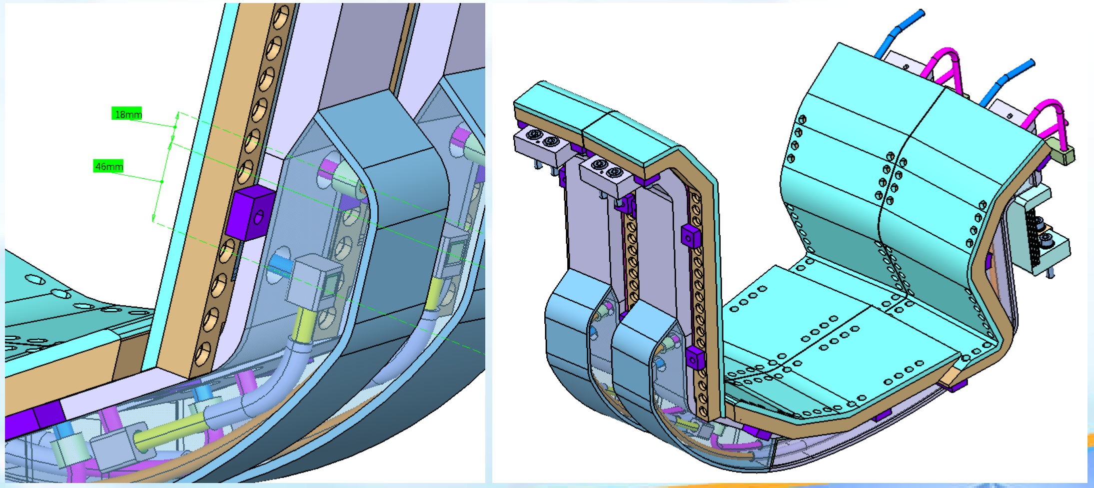

Injection location of 4 SMBI systems

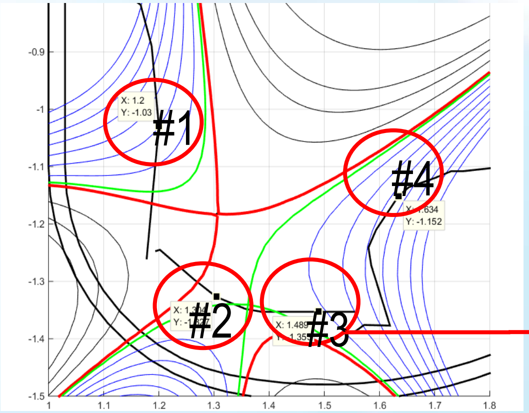

SMBI injection chamber

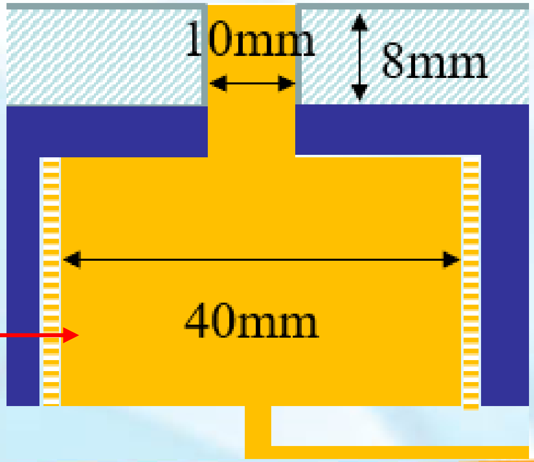

Thank you
for your attention!